Separation Science and Technology
Publication details, including instructions for authors and subscription information:
http://www.informaworld.com/smpp/title~content=t713708471

Feed Purge Cycles in Pressure Swing Adsorption

Phillip C. Wankat[a]
[a] SCHOOL OF CHEMICAL ENGINEERING, PURDUE UNIVERSITY, WEST LAFAYETTE, INDIANA

To cite this Article Wankat, Phillip C.(1993) 'Feed Purge Cycles in Pressure Swing Adsorption', Separation Science and Technology, 28: 17, 2567 — 2586
To link to this Article: DOI: 10.1080/01496399308017497
URL: http://dx.doi.org/10.1080/01496399308017497

SEPARATION SCIENCE AND TECHNOLOGY, **28**(17&18), pp. 2567–2586, 1993

Feed Purge Cycles in Pressure Swing Adsorption

PHILLIP C. WANKAT
SCHOOL OF CHEMICAL ENGINEERING
PURDUE UNIVERSITY
WEST LAFAYETTE, INDIANA 47907-1283

ABSTRACT

Three new pressure swing adsorption cycles for the production of oxygen-enriched air at very high recoveries are developed. The cycles involve a purge step using low-pressure feed gas. Local equilibrium theory is used to predict purities and recoveries for air separation with 5A zeolite. Novel methods for drying the inlet air are developed. For low product purities these processes are predicted to have very high recoveries and adsorbent productivities. A simple new method for determining the location of a curved shock wave is illustrated. Other possible applications of PSA feed purge cycles are briefly discussed.

INTRODUCTION

Pressure swing adsorption (PSA) is a well-known commercial separation method used for the separation of gases. The process was invented by Skarstrom (11) at Esso. Since that time PSA has become a commercial process for drying compressed air, separating oxygen and/or nitrogen from air, hydrogen purification, and the separation of other gases. The basic Skarstrom cycle shown in Fig. 1 consists of four steps:

1. Feed at high pressure—produce product
2. Blowdown to low pressure
3. Purge at low pressure
4. Repressurize with feed

Because of the expansion of gas when pressure is dropped, it is possible to remove all impurities during the purge step and still have a significant

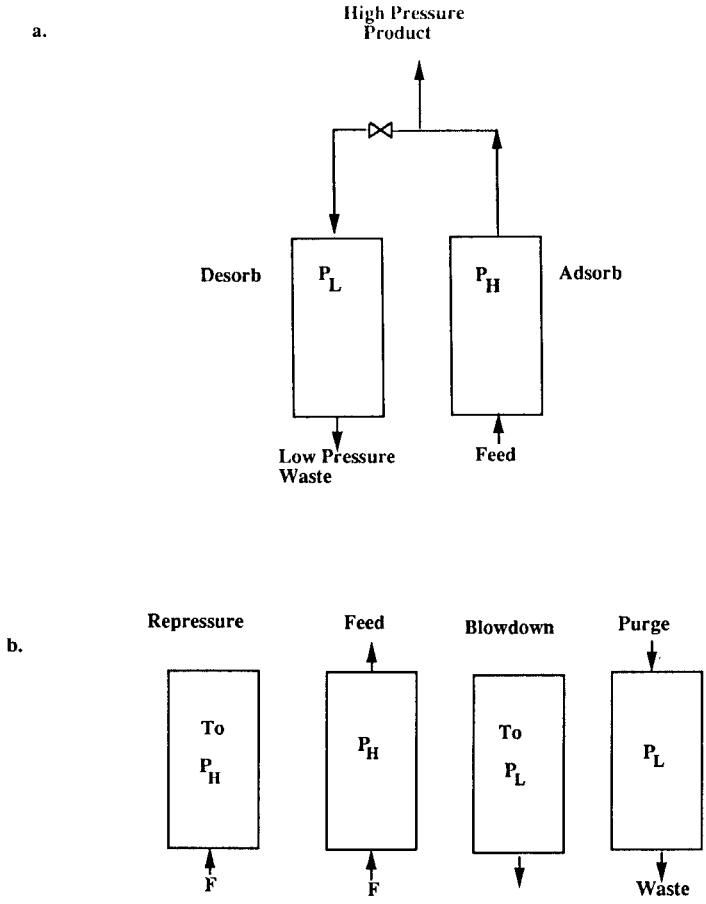

FIG. 1 Pressure swing adsorption system. a: Two-column system. b: Steps in simple PSA cycle.

amount of product. The two columns shown in Fig. 1 are operated out-of-phase with each other, and this allows continuous production of high-pressure product.

Since the first invention there have been a huge number of modifications to the basic Skarstrom cycle. These have been reviewed by Ruthven (8), Skarstrom (13), Tondeur and Wankat (14), Wankat (15), and Yang (16). Since the optimum cycle depends on the specifics of each separation problem, there are a very large number of possible sequences. The steps which

TABLE 1
PSA Steps

1. High-pressure feed	Recover high-pressure product
2. Pressurize	With feed
	With product
	With impure product
	With both feed and product
3. Blowdown	Counterflow to feed
	Coflow to feed
	Both
4. Rinse	Reflux of heavy component
5. Purge	With product
	With inert gas
	With low-pressure feed
6. Vacuum evacuation	Coflow to feed
	Counterflow to feed
	Both
	From center of bed
7. Pressure equalization	From bottom to bottom
	From top to top
	Both
8. Delay	For cycle congruence
	For mass transfer or pressure waves
9. Recycle	Impure material recycled to feed

have been identified from various papers and patents are listed in Table 1. Mixing these together in a unique way leads to a new process.

NEW CYCLES

The processes to be discussed in this paper employ a seldom used step, purge with low-pressure feed gas. Although inclusion of this step in PSA cycles will be illustrated for air separation, purge with low-pressure feed gas may also be of interest in other separations. The use of purge with low-pressure feed gas is included in a patent by Skarstrom (12) but does not appear to have been used either commercially or in other patents. Skarstrom (12) applied this to a modification of the cycle shown in Fig. 1, including a pressure equalization step.

In this paper, purge with low-pressure feed gas is combined with the cycles developed by Kratz and Sircar (5) and Sircar and Kratz (9, 10). Sircar and Kratz (10) state that one difficulty with the Skarstrom (12) cycle is the need for a source of bone-dry, CO_2-free air for the purge gas. In this paper a way to operate the process without this restriction is shown.

Kratz and Sircar (5) developed the two cycles shown in Fig. 2. The layer of desiccant dries the inlet air and removes CO_2. The main purpose of their processes was to produce low-purity oxygen from air, but, of course, these cycles may be useful for other separations. These cycles are claimed to have high recovery of compressed oxygen and high productivity.

The three related cycles developed in this paper are shown in Figs. 3, 4, and 5. Now a layer or separate column of desiccant is used at the feed end of the zeolite bed to dry and remove CO_2 from the high-pressure feed air, and a layer of desiccant or a separate column of desiccant is used to dry and remove CO_2 from the low-pressure feed purge. Use of a layer of desiccant in the same column as the zeolite is less expensive but does not allow for separate control of pressure or for bypassing the desiccant. It is not the purpose of this paper to illustrate the design of the drier layers.

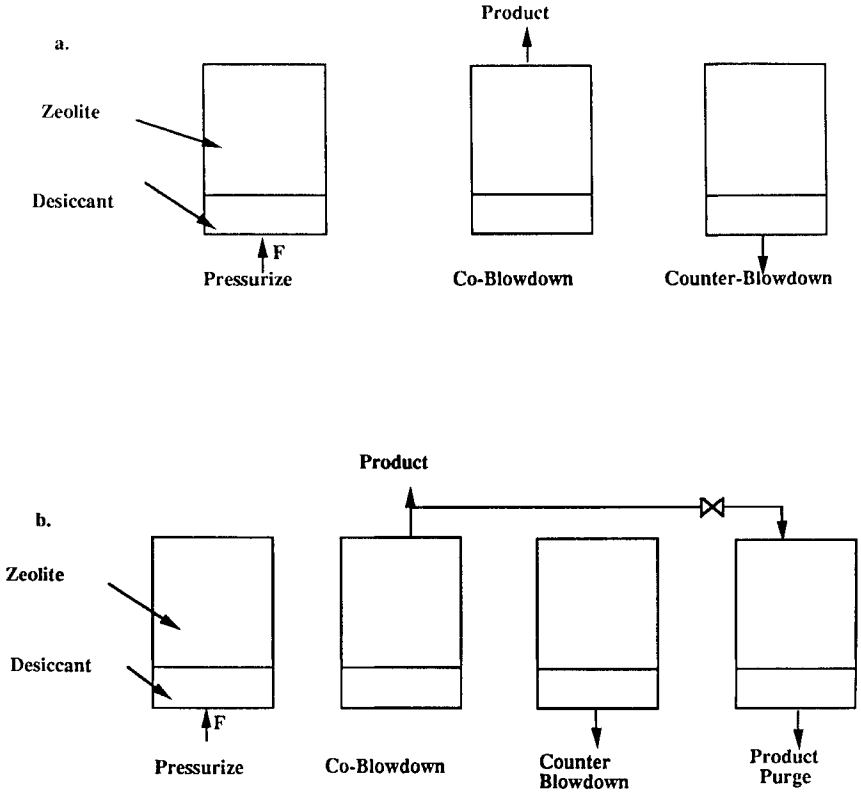

FIG. 2 Cycles for production of 23 to 50% oxygen [Sircar and Kratz (9, 10)]. a: With blowdown. b: With blowdown and product purge.

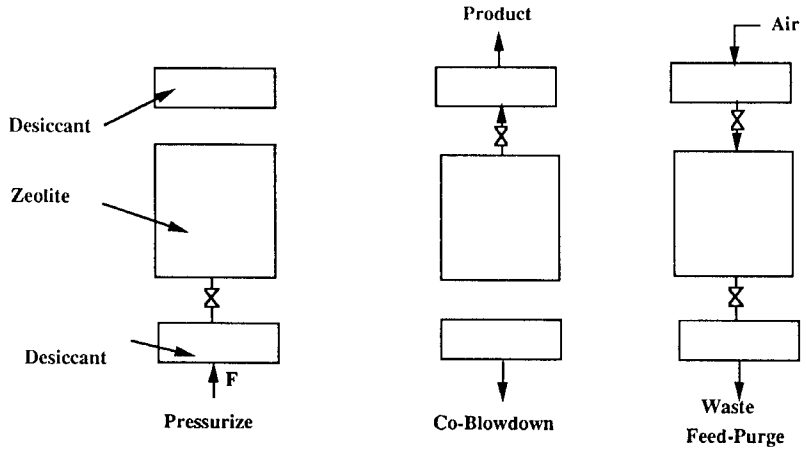

FIG. 3 New cycle with feed purge: No counterblowdown and no product purge. Compressors, valves, etc. are not shown.

If the volumetric purge to feed ratio, γ, is greater than a suitable value, it is assumed that drier operation would be satisfactory.

$$\gamma = \frac{V_{\text{purge}}}{V_{\text{feed gas}}} = \frac{P_{\text{feed}}}{P_{\text{purge}}} \frac{N_{\text{purge}}}{N_{\text{feed gas}}} \tag{1}$$

Yang (16) suggests suitable γ values are from 1.05 to 1.10, Skarstrom (13) suggests γ from 1.1 to 1.5, and a γ as high as 2.0 may be required with NaX zeolite. At a high pressure of 3 atm, all the cycles shown here can be operated with $\gamma > 1.5$ while several can be operated with $\gamma > 2.0$. In all cases shown in Figs. 3, 4, and 5, two separate desiccant columns are used. The use of two separate desiccant columns rather than desiccant layers allows one to obtain larger values of γ in the driers since the purge gas to the drier can be depressurized before entering the drier. It may be feasible to use a layer of desiccant plus a separate drying column in some cases.

Note that the product air is *not* bone-dry. The requirement to dry the air is due to the zeolite in the process. Most applications of oxygen-enriched air do not require bone-dry air, and medical applications actually rehumidify the air. Realization that the product does not have to be bone-dry air allows designs which use the product gas to regenerate the desiccant used for drying the feed purge gas.

The main feed in the column needs to be compressed. Sircar and Kratz (9, 10) report on pressures of 3.04 and 3.72 atm. Pressures as low as 1.9 atm can be used to produce 24.8% oxygen in the process shown in Fig.

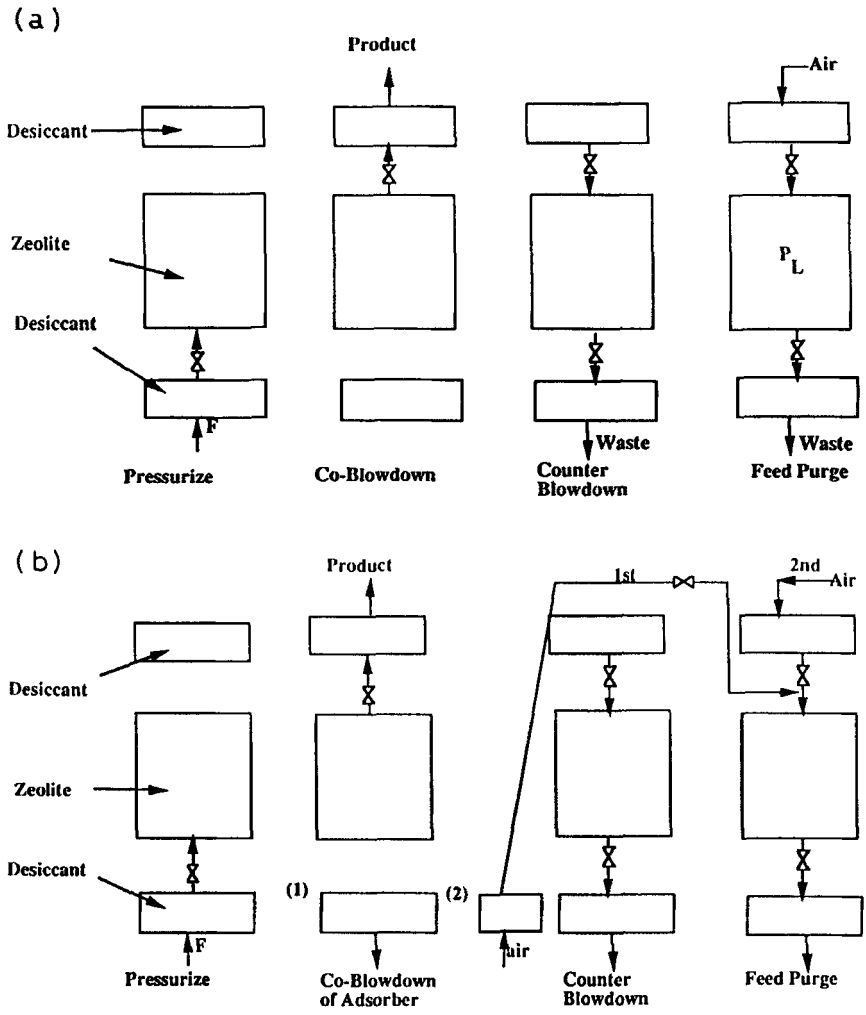

FIG. 4 New cycle with co- and counterblowdown and feed purge: No product purge. (a) Higher operating pressures. (b) Low-pressure operation. Compressors, valves, etc. are not shown.

4(a). Pressure higher than 3.7 atm will increase oxygen purity and recovery but at considerable cost for compression. The feed purge air is at low pressure and only a blower is needed. If a continuous flow of air is needed, then three or four columns are used for the cycles in Figs. 3, 4, and 5. If surging of the product air can be tolerated, a single column can be used

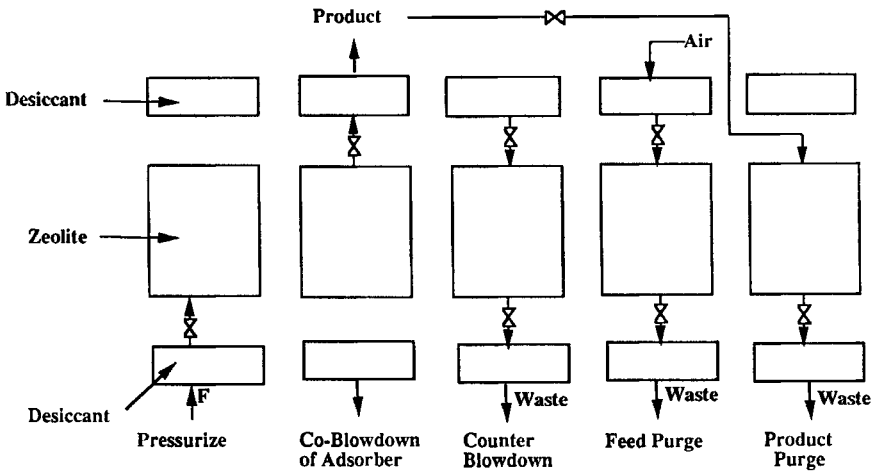

FIG. 5 New cycle with co- and counterblowdown, feed purge, and product purge. Compressors, blowers, valves, and controls are not shown.

for the cycles in Figs. 3 and 4(a). A single column plus a storage tank would be required as a minimum for the cycles in Figs. 4(b) and 5.

THEORY: PROCESSES WITHOUT SHOCKS

The cycles shown in Figs. 3, 4, and 5 have been extensively studied using the local equilibrium theory [Knaebel and Hill (4)]. Detailed experiments by Kayser and Knaebel (3) for the separation of oxygen and nitrogen in a Skarstrom cycle showed good agreement with the theoretical predictions. Thus, we have confidence that the results are reasonable. The use of the oversimplified equilibrium model allows one to study rather complex cycles without extensive computer simulations. Data for 5A zeolites was used and is shown in Table 2 [Kayser and Knaebel (3)].

TABLE 2
Data for Separation of Oxygen and Nitrogen Used in Simulations [Kayser and Knaebel (3)]

$T = 30°C = 303.16$ K, $k_{N_2} = k_{Ar} = 5.40$
$\epsilon = 0.478$, $\rho_b = 810$ g/m^3, $R = 82.057$ mol·cm^3/atm·K
$y_{N_2,F} = 0.7826$, $P_H = 3$ atm, $P_L = 1$ atm
$\beta_{N_2} = 0.08435$, $\beta_{O_2} = 0.14498$, $\beta = 0.5818$

Knaebel and Hill (4) showed that, in general, one would have both diffuse and shock waves. These occur even with linear isotherms because of variation in the gas velocity. The cycles shown in Figs. 3 and 4 are interesting since no shock waves occur. Thus, first the theory will be briefly described for diffuse waves and in the next section for shock waves. The theory assumes: instantaneous mass transfer (local equilibrium), ideal gas, negligible dispersion, negligible pressure drop, isothermal plug flow, and independent linear isotherms. Complete details are given by Knaebel and Hill (4).

Defining $\beta = \beta_A/\beta_B$ where $k_A > k_B$ and

$$\beta_i = \frac{1}{1 + \dfrac{(1 - \epsilon)k_i}{\epsilon}} \tag{2}$$

the velocity during pressurization and blowdown is

$$u = \frac{-z}{\beta_B[1 + (\beta - 1)y]} \frac{1}{P} \frac{dP}{dt} \tag{3}$$

where $z = 0$ is the closed end of the column. During constant pressure periods the velocity at Points 1 and 2 in the bed are related by

$$\frac{u_1}{u_2} = \frac{1 + (\beta - 1)y_2}{1 + (\beta - 1)y_1} \tag{4}$$

Using the method of characteristics, one obtains the following ordinary differential equations.

$$\frac{dz}{dt} = \frac{\beta_A u}{1 + (\beta - 1)y} \tag{5}$$

$$\frac{dy}{dP} = \frac{(\beta - 1)(1 - y)y}{[1 + (\beta - 1)y]P} \tag{6}$$

When pressure is constant, Eq. (6) implies y is constant along the characteristics given by Eq. (5). When pressure varies from initial condition "0," these equations can be integrated to give

$$\frac{y}{y_0} = \left(\frac{1 - y}{1 - y_0}\right)^{\beta} \left(\frac{P}{P_0}\right)^{\beta - 1} \tag{7}$$

$$\frac{z}{z_0} = \left(\frac{y}{y_0}\right)^{\beta/1 - \beta} \left(\frac{1 - y_0}{1 - y}\right)^{1/1 - \beta} \left(\frac{1 + (\beta - 1)y}{1 + (\beta - 1)y_0}\right) \tag{8}$$

During pressurization the moles of feed entering the column is

$$N_{PR} = -\int_0^{t_{PR}} u_{PR} \frac{P}{RT} \epsilon A_{cs}\, dt \tag{9}$$

where u_{PR} comes from Eq. (3). The result is

$$N_{PR} = \frac{\epsilon A_{cs} L(P_H - P_L)}{\beta_B RT[1 + (\beta - 1)y_F]} \tag{10}$$

During blowdown

$$N_{BD} = \int_0^{t_{BD}} u_{BD} \frac{P}{RT} \epsilon A_{cs}\, dt \tag{11}$$

where u_{BD} comes from Eq. (3).

$$N_{BD} = \int_{P_H}^{P_L} \frac{L\epsilon A_{cs}}{\beta_B[1 + (\beta - 1)y]RT}\, dP \tag{12}$$

Unfortunately, y varies as shown by Eqs. (7) and (8). The integral is easily evaluated numerically. The moles of N_2 in the blowdown is easily obtained by multiplying the integrand by y.

If we are willing to require that the feed purge step convert the entire column to mole fraction y_F, then cyclic steady-state results can be obtained immediately. Since this greatly simplifies the calculations, we will do this; however, in actual practice, less feed purge can be used. With this requirement the entire column is at y_F and P_L for the start of the pressurization step. Since the pressurizing gas is at y_F, no shock wave occurs. The resulting characteristic diagram for the process in Fig. 3 is shown in Fig. 6. The numerical values in this figure are for $P_L = 1$ and

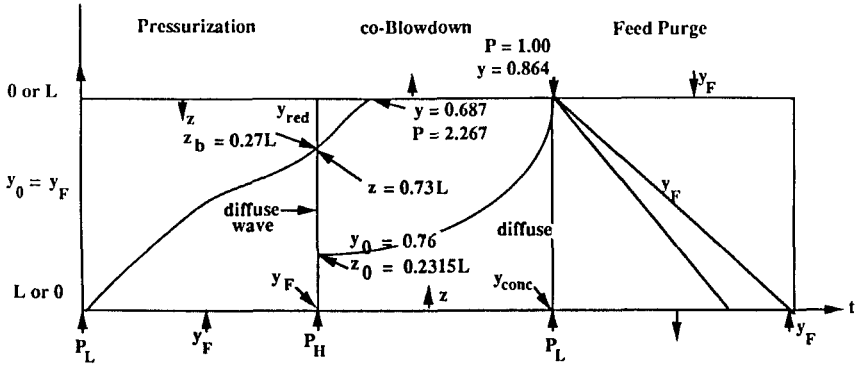

FIG. 6 Characteristic diagram at cyclic steady-state for processes in Fig. 3. Conditions are given in Table 2.

$P_H = 3$, but the shape of the diagram will be unchanged for other pressures or y_F values.

For $y_0 = y_F$, $P_0 = P_L = 1$ and $P = P_H = 3$, Eq. (7) can be solved for $y = y_{red}$. For the oxygen–nitrogen values in Table 2, the result is $y_{red} = 0.651$. This value helps to explain why the process in Fig. 3 will produce oxygen-enriched air. More nitrogen is adsorbed when the column is pressurized, and thus the oxygen content of the air increases (y_{N_2} decreases). The ending location of the characteristic starting at $t = 0$ can be found from Eq. (8) with $y_0 = y_{red}$ and $y = y_F$. The value of y at any value of z at the end of the pressurization step can also be found from Eq. (8). The values obtained can be checked with an overall mass balance around the column for the pressurization step.

$$N_{PR} = A_{cs}L\epsilon\frac{(P_H - P_L)}{RT} + A_{cs}z_b(1 - \epsilon)\frac{P_H}{RT}[k_{O_2}(1 - y_{red}) + k_{N_2}y_{red}]$$
$$+ A_{cs}L(1 - \epsilon)\frac{P_H}{RT}(-1)\int_L^{z_b}[k_{O_2}(1 - y) + k_{N_2}y]$$
$$\times dz - A_{cs}L(1 - \epsilon)\frac{P_L}{RT}[k_{O_2}(1 - y_F) + k_{N_2}y_F] \quad (13)$$

On the right-hand side, the first term is final minus initial states for the gas, the second term is the final amount adsorbed down to the "border" wave representing the feed characteristic, the third term is the amount adsorbed in the diffuse wave, and the last term is the initial amount adsorbed. This equation is simplified since $k_{O_2} = k_{Ar}$, and the oxygen and argon can be lumped together. The integral is easily determined numerically. It could also be determined by substituting Eq. (8) into Eq. (13), but this is algebraically messy. The nitrogen mass balance can also be used.

The calculation for blowdown uses the end of the pressurization step as the initial condition. Note that z must be shifted. N_{BD} can be obtained numerically from Eq. (12) where y is related to P by Eq. (7) and y_0 corresponds to the y values at the end of the pressurization step at specified z_0. This can be done conveniently by setting $z = L$ in Eq. (8) and then solving for y which is the outlet gas starting from a specified point (y_0, z_0) in the column. The outlet pressure P is then determined from Eq. (7), and Eq. (12) can be integrated. The last characteristic exiting the column ($P = P_L = 1.00$) is also shown. Concentrations for the diffuse wave at the end of the blowdown step are done by using Eq. (7) with $P/P_0 = 3/1$ to find y, and then using Eq. (8) to find z. At $z = 0$, $y_{conc} = 0.879$ is the highest nitrogen concentration obtained in this cycle.

Since the diffuse wave inside the column at the end of the blowdown step has more nitrogen than air, it is advantageous to use feed air at P_L to purge the column. A diffuse wave results. It was timed so that the entire column was at y_F at the end of the feed purge step. From Eq. (5),

$$L = \frac{\beta_A u_{Pu} t_{Pu}}{1 + (\beta - 1) y_F} \tag{14}$$

and then

$$N_{Pu,in} = u_{Pu} \frac{P_L}{RT} \epsilon A_{cs} t_{Pu} = \frac{A_{cs} L \epsilon P_L [1 + (\beta - 1) y_F]}{RT \beta_{N_2}} \tag{15}$$

The exiting concentrations during the purge step can be determined by following characteristics which start at the diffuse wave from the end of blowdown. Alternatively, the average concentrations exiting during the feed purge step can be obtained from a mass balance over the entire cycle. Once nitrogen mole fractions are obtained,

$$y_{Ar} + y_{O_2} = 1 - y_{N_2} \tag{16}$$

The oxygen mole fraction was obtained by requiring [Islaski (2)]

$$\frac{y_{O_2}}{y_{O_2} + y_{Ar}} = 0.9573 \tag{17}$$

The cycle shown in Figure 3 does not have an equivalent in the scheme of Sircar and Kratz (9, 10). Our calculations predicted a product which is 24.4% oxygen for a high pressure of 3 atm. Recovery of oxygen from all input air was 81.9% while recovery of oxygen in compressed air was 113.8%. This recovery is greater than 100% since some of the oxygen in the product came from the feed-purge air. Since the major operating cost is the compressor operation, reporting recovery based on oxygen in the compressed gas is a reasonable way to compare processes. The outlet drier in Fig. 3 can be operated with $\gamma > 2.0$ by reducing the product pressure. The inlet drier operates at $\gamma \approx 1.2$ if $P_{waste} = 1.0$. According to some authors, this γ may not be large enough to obtain complete drying of the inlet air. Additional feed purge gas beyond that shown in Fig. 6 can be used to help purge the inlet drier. By adjusting the amount of feed purge gas used, a maximum γ of 1.7 can be obtained in each drier if the product gas and waste gas are at 1 atm. If $\gamma = 1.5$ is sufficient, higher pressures can be used for product and/or waste streams.

During the latter part of the coblowdown step in the cycle shown in Fig. 3, the gas going into the product contains less oxygen than air. Thus, it is reasonable to stop the coblowdown step when the product gas has

approximately the same composition as air. A counterblowdown step is added as shown in Fig. 4. The characteristic diagram for these processes is shown in Fig. 7. The feed purge step is again controlled by the characteristic line at y_F. Then the pressurization step is the same as in Fig. 6. The coblowdown step is the same as in Fig.6 except it ends earlier (at y = 0.784, P_m = 1.71 atm). The calculations for the counterblowdown step are initialized with the final conditions for coblowdown. This is shown for one example characteristic. With a high pressure of 3 atm this scheme produced an oxygen gas which was 28.8% oxygen at a recovery of 61% of all oxygen input and 84.7% of oxygen in the compressed gas. A $\gamma >$ 1.5 can be obtained for the outlet drier while $\gamma > 2.0$ for the inlet drier. These values are sufficient for a drier using activated alumina. If a higher purity is required, the coblowdown step can be stopped at a higher pressure. For instance, a 31.7% oxygen product can be obtained at a recovery of 37.3% of the oxygen in all input air (51.8% of oxygen in compressed air). These recoveries (37.3 and 51.8%) are low, and the scheme shown in Fig. 5 becomes preferable.

The effect of pressure on the cycles shown in Fig. 4 was studied. In these cases the coblowdown step was stopped when the exiting gas had the same composition as air. These results are shown in Table 3. These results represent the "natural" operation of this cycle. If a lower oxygen purity is desired, it can be obtained by mixing product with air. The last column in Table 3 gives recoveries if the product is mixed with air to give a 25% oxygen product. Obviously, a blower is needed for the air that will be mixed with the blowdown product. As the pressure is decreased, it becomes increasingly more difficult to totally regenerate the outlet drier

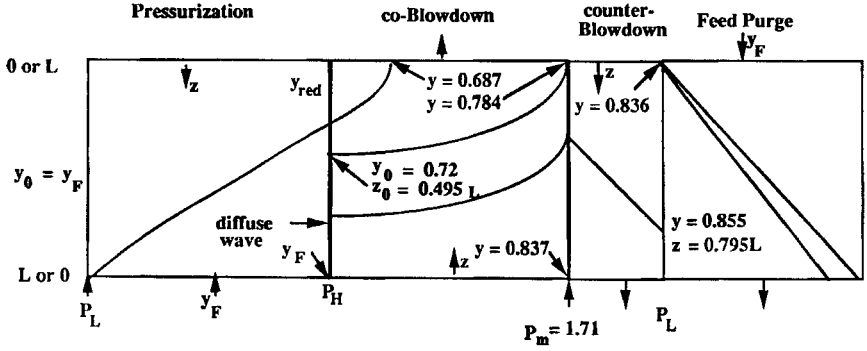

FIG. 7 Characteristic diagram at cyclic steady-state for processes in Fig. 4. Conditions are given in Table 2.

TABLE 3
Theoretical Results for Pressure Effects on Cycle Shown in Figure 4a or 4b

P_H (atm)	O_2 mole fraction in product (%)	Highest delivery pressure of product (atm)	O_2 recovery of all inlet air (%)	O_2 recovery of compressed air (%)	Recovery of compressed O_2 if mixed to 25% (%)
6	31.4	3.4	57.1	65.9	135.9
3.0	28.8	1.7	61	84.7	143.3
2.2	25.2	1.24[b]	58.2	95.9	117.8
1.9[a]	24.8	1.07	56.6	105.5	—

[a] Cycle in Fig. 4b must be used.
[b] This delivery pressure is possible only if the cycle in Fig. 4b is used.

(used to dry the feed purge gas). The use of the scheme in Fig. 4(b) will allow operation at lower pressures or at higher γ values in the outlet drier.

THEORY: PROCESS WITH SHOCK WAVES

For higher product purities the cycle shown in Fig. 5 will give higher recoveries than the simple cycles. In this cycle a product purge is used after the feed purge step. This adds additional complexity to the process and an additional step to optimize.

For this process a shock wave results during the pressurization step because material at y_F displaces the product purge material. Knaebel and Hill (4) showed that for the pressurization and blowdown steps the shock wave velocity is

$$u_{sh} = \frac{-\beta z}{(1 + (\beta - 1)y_1)(1 + (\beta - 1)y_2)} \frac{1}{P} \frac{dP}{dt} \tag{18}$$

while at constant pressure

$$u_{sh} = \frac{\beta_A u_1}{1 + (\beta - 1)y_2} = \frac{\beta_A u_2}{1 + (\beta - 1)y_1} \tag{19}$$

where 1 denotes material immediately in front of the shock and 2 is material immediately behind the shock. In general, the shock wave curves. Knaebel and Hill (4) illustrate a fairly difficult procedure for following the path of the shock wave. We will satisfy the overall mass balance for the step to find the shock location indirectly.

The cyclic steady-state can be determined without the need for startup equations. Again, require that the feed end of the column be regenerated

to the feed mole fraction, y_F. Pick the desired ratio of feed purge to total purge, N_{FP}/N_{Pu}. Then $N_{PP}/N_{Pu} = 1 - (N_{FP}/N_{Pu})$. Set the required value of total product mole fraction y_P. One can now start with the feed purge and product purge steps. Then the pressurization step, including the shock wave, can be calculated. The coblowdown step is done to an intermediate pressure P_m at which the average coblowdown product composition equals y_P. The counterblowdown procedure is then essentially the same as in Fig. 7.

The calculations for the processes shown in Fig. 5 are shown in Fig. 8 for $y_P = 0.67$ ($y_{0_2} + y_{Ar} = 0.33$ or $y_{0_2} = 0.316$) with 70% of the purge being feed purge. This diagram is similar to Figs. 6 and 7 except it is convenient to show the purge step first. Assuming a constant inlet purge gas velocity, u_{Pu}, the total purge time t_{Pu} is again determined by Eq. (14) since the y_F characteristic is unchanged by switching from feed purge to product purge. From Eq. (5) the relative velocities at $y = y_F$ and $y = y_P = 0.67$ can be determined. It is then easy to calculate that the diffuse wave extends from $z = 0.28035L$ to $z = 0.30L$ at the end of the product purge.

During the repressurization step the diffuse wave first reversibly reforms a step change (the local equilibrium theory has ignored irreversible mass transfer and dispersion) and then a curved shock wave forms. This is sketched approximately in Fig. 8. The exact location of the shock wave at the end of the pressurization step can be found from a mass balance around the pressurization step. The remaining calculations for the pressur-

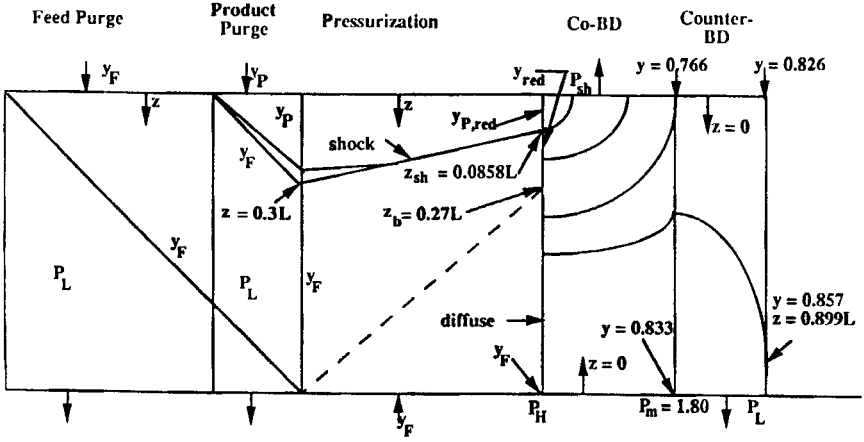

FIG. 8 Characteristic diagram at cyclic steady-state for process in Fig. 5. Conditions are listed in Table 2. $y_P = .67$, $N_{FP}/N_{Pu} = 0.7$.

ization step are exactly like those in Figs. 6 and 7. The gas above the shock wave started at y_P and is pressurized to $P_H = 3$. Following Eq. (7), one obtains $y_{P,red} = 0.5238$. Below the shock wave the gas went from y_F to $y_{red} = 0.651$.

The mass balance around the pressurization step is

$$N_{Pr} = A_{cs}L\epsilon\frac{P_H - P_L}{RT} + A_{cs}z_{sh}\frac{P_H}{RT}(1 - \epsilon)$$
$$\times [k_{O_2}(1 - y_{P,red}) + k_{N_2}y_{P,red}]$$
$$+ (1 - \epsilon)A_{cs}\frac{P_H}{RT}(z_b - z_{sh})[k_{O_2}(1 - y_{red}) + k_{N_2}y_{red}]$$
$$+ (1 - \epsilon)A_{cs}\frac{P_H}{RT}\int_L^{z_b}[k_{O_2}(1 - y) + k_{N2}y]$$
$$\times dz - (1 - \epsilon)\frac{A_{cs}P_L}{RT}[0.7L(k_{O_2}(1 - y_F) + k_{N_2}y_F)$$
$$+ \int_{0.3L}^{0.28035L}[k_{O_2}(1 - y) + k_{N_2}y]dz + 0.28035L$$
$$\times [k_{O_2}(1 - y_F) + k_{N_2}y_P] \tag{20}$$

In Eq. (20) the first term is again the final minus initial amount of pore gas; the second to fourth terms are the final amounts adsorbed above the shock wave, between the shock and the border wave, and in the diffuse wave; and the subtracted term represents the initial amount adsorbed below the diffuse wave, in the diffuse wave, and above the diffuse wave. The two integrals are easily determined numerically (the first one is exactly the same as in Eq. 13). Equation (20) is linear in z_{sh}, which allows for a simple determination of z_{sh}.

The final state for pressurization is the initial state for coblowdown. Everything below the shock wave is exactly the same in Fig. 8 as in Figs. 6 and 7. This obviously eases the calculations. The coblowdown calculations are complicated by the shock wave. The initial condition for the shock is $z_{sh,0} = 1 - z_{sh} = 0.9142L$ since $z = 0$ is now the feed end of the column. Equation (8) is used to go from $z_{sh,0}$ to $z = L$ for concentrations on both sides of the shock wave. Then Eq. (7) is used to calculate P at the outlet. This shows a jump in pressure. Since a pressure jump probably causes an error in the calculation of N_{BD} from Eq. (12), the average pressure was used as the shock wave pressure ($P_{sh} = 2.75$ atm). The error introduced by this approximate calculation should be small.

TABLE 4
Results from Calculations for Cycle in Figure 5

% O_2 in product	% Product purge of total purge	Recovery of oxygen in compressed gas (%)	Recovery of oxygen in total air fed to process (%)
31.6	20	65.9	47.4
	30	67.0	48.3
	40	58.7	42.3
38.2	20	29.4	22.4
	50	46.1	38.6
	70	47.8	42.8
	90	52.6	50.6

The remainder of the coblowdown calculation is the same as those done in Fig. 7. Now P_m is shown so that

$$y_P = \frac{N_{BD,N_2}}{N_{BD}} \tag{21}$$

$$y_P = \frac{\int_{P_H}^{P_m} \frac{L\epsilon A_{cs} y}{\beta_{O_2}[1 + (\beta - 1)y]RT}\, dP}{\int_{P_H}^{P_m} \frac{L\epsilon A_{cs}}{\beta_{O_2}[1 + (\beta - 1)y]RT}\, dP} \tag{22}$$

This is a straightforward numerical calculation. This step is necessary since y_P was chosen to start the purge calculation.

The counterblowdown step is essentially the same as in Fig. 7. The same starting characteristic as calculated in Fig. 7 is shown in Fig. 8. It moves closer to the outlet in Fig. 8 since the counterblowdown step is longer.

The results from two sets of calculations are given in Table 4. The total amount of purge has not been optimized. The high pressure was 3 atm and the low pressure 1 atm in all calculations. For the 31.6% oxygen product with 30% product purge, both driers can easily operate with $\gamma > 1.5$. If the product delivery pressure is reduced to 1 atm, both driers can operate with $\gamma > 2.0$. Thus, producing dry air should not be a problem.

DISCUSSION

The obvious question is: Are the results obtained good or bad? An approximate comparison can be made with the pilot-plant results of Sircar and Kratz (9, 10) for the processes shown in Fig. 2. They used zeolite X

which is better in this application than 5A. Despite this, a qualitative comparison can be made. For a 25% oxygen product the process shown in Fig. 2(a) had about 80% recovery. The results shown in Table 3 show a significantly higher recovery of oxygen in the compressed gas (except at $P_H = 6$) and a significantly higher recovery if the product is mixed to produce a 25% oxygen product. When product purge is used (Fig. 2b or 5), the results in Table 4 can be compared to Sircar and Kratz (9, 10). At 31.6% oxygen, Sircar and Kratz (9, 10) had about 64% recovery with $P_H = 3.04$ atm. For 38.2% oxygen, they obtained about 55% recovery. Thus, for low-purity oxygen the cycles shown in Figs. 3 and 4 appear to have an advantage. When product purge is used to obtain higher oxygen mole fractions, the use of feed purge in addition is advantageous at low oxygen concentrations (e.g., 31.6%) but probably is not useful at higher oxygen concentrations. Note that the processes shown in Figs. 3, 4, and 5 will usually require two separate drier beds for each adsorption column, but Sircar and Kratz's process (Fig. 2) requires only a single layer of desiccant in the adsorption column. In addition, the Sircar and Kratz process has been completely tested experimentally while the processes shown here have not been tested experimentally. Thus, the appropriate conclusion is that the feed purge processes have promise and should be tested experimentally.

Feed purge may be useful in other cycles for oxygen production. For example, one can include a high-pressure feed step with product withdrawal before the coblowdown in the cycles shown in Figs. 3 to 5. The cycles studied by Liow and Kenney (6) can also be adapted to include a feed purge step as shown in Fig. 9. For simplicity, the drier beds are not

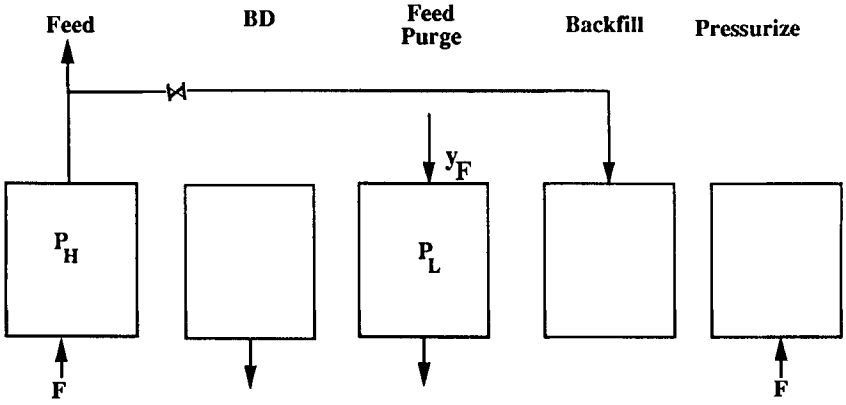

FIG. 9 Inclusion of feed purge step in cycle of Liow and Kenney (6). Desiccant beds, compressors, valves, etc. are not shown.

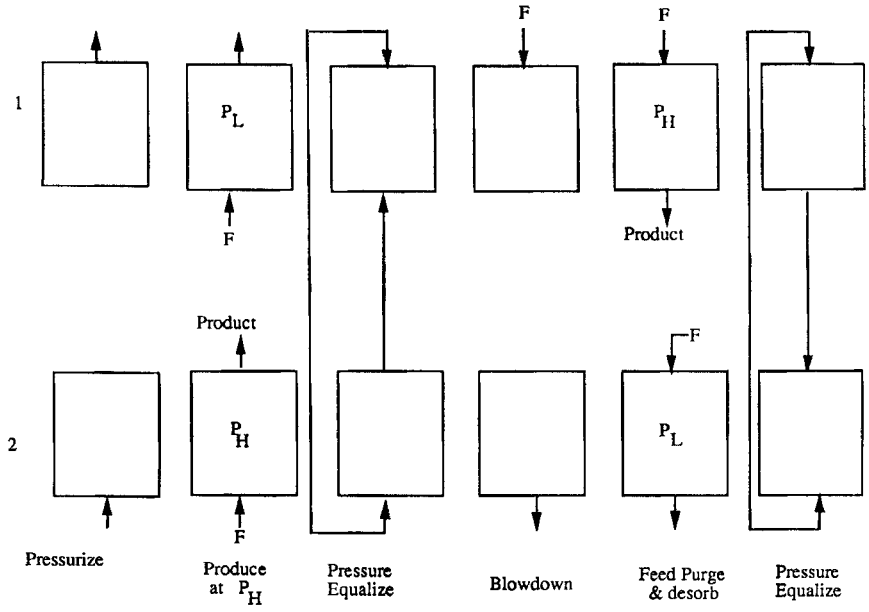

FIG. 10 Proposed use of feed purge in cycle for N_2 separation from air. Two columns are used as shown. Steps are labeled for Column 2. Desiccant beds, compressors, valves, etc. are not shown.

shown for this cycle. Since this cycle normally operated without a purge step and produced low-purity oxygen, the introduction of a feed purge step may cause the same major increase in oxygen recovery as for the cycle in Fig. 2(a). The model employed here could easily be applied to this cycle.

Feed purge may also be useful for other gas separations when a pure product is not required. A specific example is the production of 95 to 96% nitrogen from air using a carbon molecular sieve. The proposed modified process is shown in Fig. 10 without appropriate drier beds. Current practice uses this cycle without the feed purge step (there is a separate desorb step instead) [Hassan et al. (1), Pilarczyk and Knoblauch (7)]. Since this is a kinetic-based separation, the model used to study the oxygen separation is not applicable. A more detailed analysis is needed to study the applicability of the feed purge step in this case.

One application where feed purge would not be applicable is drying compressed air. Since water is normally removed as condensate after each compression step, $y_{amb} > y_F$. Thus, there is no convenient source of low pressure "feed" gas to use for the feed purge.

NOTATION

A_{cs}	cross-sectional area of column (m^2)
k_i	linear equilibrium constant [(mol/m^3 solid)/(mol/m^3 gas)]
L	column length (m) [Note: Knaebel and Hill (4) used $L = 1$]
N_{BD}	moles blowdown gas
N_{PR}	moles pressurization gas
$N_{Pu,in}$	moles inlet purge gas
N	moles
N_{PP}	moles product purge
P	pressure (atm)
P_H	high pressure (atm)
P_L	low pressure (atm)
P_m	medium pressure—border between co- and counterblowdown steps (atm)
R	gas constant
t	time (second)
T	temperature (K)
u	velocity (m/s)
u_{sh}	shock velocity (m/s)
V	volume (m^3)
y	mole fraction A (more strongly adsorbed = N_2)
y_F	feed mole fraction
y_P	product mole fraction
z	axial distance (m)
z_b	"border" wave for feed (m)
z_{sh}	location of shock wave (m)

Greek

β	β_A/β_B
β_i	Eq. (2)
ϵ	porosity
γ	$V_{purge}/V_{feed\ gas}$. Volumetric purge-to-feed ratio

ACKNOWLEDGMENT

This research was done at the Department of Chemical Engineering, University of Florida, while the author was on sabbatical. Their hospitality is gratefully acknowledged.

REFERENCES

1. M. M. Hassan, N. S. Raghavan, and D. M. Ruthven, "Pressure Swing Air Separation on a Carbon Molecular Sieve—II. Investigation of a Modified Cycle with Pressure Equalization and No Purge," *Chem. Eng. Sci.*, *42*, 2037 (1987).
2. W. H. Islaski, *Separation of Gases*, Oxford University Press, Oxford, 1989.
3. J. C. Kayser and K. S. Knaebel, "Pressure Swing Adsorption: Experimental Study of an Equilibrium Theory," *Chem. Eng. Sci.*, *41*, 2931 (1986).
4. K. S. Knaebel and F. B. Hill, "Pressure Swing Adsorption: Development of an Equilibrium Theory for Gas Separations," *Ibid.*, *40*, 2351 (1985).
5. W. C. Kratz and S. Sircar, U.S. Patent 4,685,939 (1987).
6. J.-L. Liow and C. N. Kenney, "The Backfill Cycle of the Pressure Swing Adsorption Process," *AIChE J.*, *36*, 53 (1990).
7. E. Pilarczyk and K. Knoblauch, "Gas Separation Processes by Pressure Swing Adsorption Using Carbon Molecular Sieves," in *Separation Technology* (N. N. Li and H. Strathman, Eds.), Engineering Foundation, New York, 1988, p. 522.
8. D. M. Ruthven, *Principles of Adsorption and Adsorption Processes*, Wiley, New York, 1984.
9. S. Sircar and W. C. Kratz, "The Oxy-rich Pressure Swing Adsorption Process for Production of Oxygen Enriched Air," *AIChE Symp. Ser.*, *84*(264), 141 (1988).
10. S. Sircar and W. C. Kratz, "A Pressure Swing Adsorption Process for Production of 23–50% Enriched Air," *Sep. Sci. Technol.*, *23*, 437 (1988).
11. C. W. Skarstrom, U.S. Patent 2,944,627 (July 12, 1960).
12. C. W. Skarstrom, U.S. Patent 3,237,377 (March 1, 1966).
13. C. W. Skarstrom, "Heatless Fractionation of Gases over Solid Adsorbents," in *Recent Developments in Separation Science*, Vol. II (N. N. Li, Ed.), CRC Press, Boca Raton, Florida, 1972, p. 95.
14. D. Tondeur and P. C. Wankat, "Gas Purification by Pressure Swing Adsorption," *Sep. Purif. Methods*, *14*, 157 (1985).
15. P. C. Wankat, *Large Scale Adsorption and Chromatography*, CRC Press, Boca Raton, Florida, 1986.
16. R. T. Yang, *Gas Separation by Adsorption Processes*, Butterworths, Boston, 1987.

Received by editor July 6, 1992
Revised May 12, 1993